

## ***Electronic Supplementary Information***

### **Luminescent Modulation, Near White Light Emission, Selective Luminescence Sensing, and Anticounterfeit via a Series of Ln-MOFs with $\pi$ -Conjugated and Uncoordinated Lewis Basic Triazolyl Ligand**

Lu-Lu Ma, Guo-Ping Yang\*, Gao-Peng Li, Peng-Feng Zhang, Jing Jin, Yao Wang,  
Jiao-Min Wang and Yao-Yu Wang\*

Key Laboratory of Synthetic and Natural Functional Molecule of the Ministry of  
Education, Shaanxi Key Laboratory of Physico-Inorganic Chemistry, College of  
Chemistry & Materials Science, Northwest University, Xi'an, 710127, Shaanxi, P. R.  
China. E-mail: [ygp@nwu.edu.cn](mailto:ygp@nwu.edu.cn); [wyaoyu@nwu.edu.cn](mailto:wyaoyu@nwu.edu.cn).

# Contents

Section S1. Materials and General Methods.

Table S1. Selected bond lengths (Å) and bond angles (°) for **1-Eu**, **1-Tb** and **1-Gd**.

Table S2. Summary of the quantum yields of the reported white-light-emission doped MOFs.

Table S3. The quenching constants of **1-Eu** and reported MOFs for NB.

Table S4. Results of ICP analyses of  $\text{Eu}^{3+}$ .

Figure S1. Coordination geometry of  $\text{Eu}^{3+}$  in **1-Eu**, (a) a distorted trigondodecahedron geometry (b) a distorted tetrakaidecahedron geometry.

Figure S2. Three coordination modes of  $\text{L}^{2-}$  in **1-Eu**.

Figure S3. PXRD patterns of **1-Eu** simulated from the X-ray single-crystal structure and as-synthesized samples of **1-Eu**, **1-Tb** and **1-Gd**.

Figure S4. PXRD patterns of doped samples.

Figure S5. The TGA plots of **1-Eu**, **1-Tb** and **1-Gd** under  $\text{N}_2$  environment.

Figure S6. The FT-IR spectrometer of **1-Eu**, **1-Tb** and **1-Gd**.

Figure S7. Solid state excitation spectra of  $\text{H}_2\text{L}$  (a), **1-Gd**(b), **1-Eu**(c) and **1-Tb**(d).

Figure S8. Solid-state emission spectra of  $\text{H}_2\text{L}$ (a), **1-Gd** (b).

Figure S9. Luminescence decay lifetimes of **1-Eu**(a), **1-Tb**(b) and **1-Gd**(c) measured at the excitation.

Figure S10. Linear correlation for the plot of  $(I_0/I)-1$  vs concentration of nitrobenzene in low concentration range.

Figure S11. UV-Vis adsorption spectrum of  $\text{H}_2\text{L}$ , and the excitation spectrum of **1-Eu**.

Figure S12. The PXRD patterns of **1-Eu** treated by small organic molecules solution.

Figure S13. The PXRD patterns of **1-Eu** treated by multi-cycle fluorescence quenching.

**Section S1. Materials and General Methods.** All materials were purchased commercially and used directly without any treatment. Thermogravimetric analysis (TGA) was performed on a NETZSCH STA 449C equipment under a N<sub>2</sub> atmosphere (10 °C min<sup>-1</sup>). Powder X-ray diffraction (PXRD) was carried out on a Bruker D8 ADVANCE powder X-ray diffractometer with Cu-K $\alpha$  radiation ( $\lambda=1.5418$  Å) at room temperature. Fourier transform infrared (FT-IR) spectroscopy was recorded as KBr pellets on an EQUINOX55 FT-IR spectrometer in 4000-400 cm<sup>-1</sup>. Elemental analyses (C, H, and N) were obtained with a PerkinElmer 2400C elemental analyzer. Luminescent spectra were determined on an Edinburgh FLS920 fluorescence spectrometer. UV-vis spectroscopic data were collected on a Hitachi U-3310 spectrometer. The quantum efficiency was tested by an integrating sphere on a FluoroMax-4 spectrophotometer.

**Table S1.** Selected bond lengths (Å) and bond angles (°) for **1-Eu**, **1-Tb** and **1-Gd**.

<b>1-Eu</b>			
Eu(1)-Eu(2)	4.0710(4)	Eu(2)-O(4)#3	2.5059(17)
Eu(1)-O(7)#1	2.3347(18)	Eu(2)-O(12)#4	2.4327(19)
Eu(1)-O(1)	2.5994(18)	Eu(2)-O(5)	2.4424(17)
Eu(1)-O(5)	2.5453(18)	Eu(2)-O(3)#3	2.3848(19)
Eu(1)-O(10)#1	2.3615(19)	Eu(2)-O(11)#4	2.4309(19)
Eu(1)-O(2)	2.4748(19)	O(7)-Eu(1)#4	2.3346(18)
Eu(1)-O(6)	2.5601(18)	O(8)-Eu(2)#4	2.3188(18)
Eu(1)-O(13)	2.412(2)	O(4)-Eu(2)#3	2.5059(17)
Eu(1)-N(3)#2	2.571(2)	O(12)-Eu(2)#1	2.4329(19)
Eu(1)-O(14)	2.378(3)	O(3)-Eu(2)#3	2.3849(19)
Eu(2)-O(9)	2.3050(18)	O(10)-Eu(1)#4	2.3616(18)
Eu(2)-O(8)#1	2.3189(18)	O(11)-Eu(2)#1	2.4309(19)
Eu(2)-O(1)	2.4257(17)	N(3)-Eu(1)#2	2.571(2)
O(7)#1-Eu(1)-Eu(2)	64.65(5)	O(14)-Eu(1)-O(13)	144.10(9)
O(7)#1-Eu(1)-O(1)	76.43(6)	O(14)-Eu(1)-N(3)#2	88.98(12)
O(7)#1-Eu(1)-O(5)	81.27(6)	O(9)-Eu(2)-Eu(1)	104.77(4)
O(7)#1-Eu(1)-O(10)#1	82.05(7)	O(9)-Eu(2)-O(8)#1	81.93(7)
O(7)#1-Eu(1)-O(6)	129.43(6)	O(9)-Eu(2)-O(1)	141.66(6)
O(7)#1-Eu(1)-O(13)	80.45(8)	O(9)-Eu(2)-O(4)#3	74.15(6)
O(7)#1-Eu(1)-N(3)#2	152.05(7)	O(9)-Eu(2)-O(12)#4	121.97(6)
O(7)#1-Eu(1)-O(14)	86.33(11)	O(9)-Eu(2)-O(5)	78.22(6)
O(1)-Eu(1)-Eu(2)	34.48(4)	O(9)-Eu(2)-O(3)#3	126.76(6)
O(5)-Eu(1)-Eu(2)	34.47(4)	O(9)-Eu(2)-O(11)#4	88.87(7)
O(5)-Eu(1)-O(1)	65.03(6)	O(8)#1-Eu(2)-Eu(1)	68.37(5)
O(5)-Eu(1)-O(6)	51.07(5)	O(8)#1-Eu(2)-O(1)	77.40(6)
O(5)-Eu(1)-N(3)#2	124.07(6)	O(8)#1-Eu(2)-O(4)#3	77.83(6)
O(10)#1-Eu(1)-Eu(2)	146.70(5)	O(8)#1-Eu(2)-O(12)#4	149.01(6)

O(10)#1-Eu(1)-O(1)	139.62(6)	O(8)#1-Eu(2)-O(5)	88.13(6)
O(10)#1-Eu(1)-O(5)	144.13(6)	O(8)#1-Eu(2)-O(3)#3	79.26(7)
O(10)#1-Eu(1)-O(2)	129.77(7)	O(8)#1-Eu(2)-O(11)#4	154.76(6)
O(10)#1-Eu(1)-O(6)	125.28(7)	O(1)-Eu(2)-Eu(1)	37.35(4)
O(10)#1-Eu(1)-N(3)#2	70.33(7)	O(1)-Eu(2)-O(4)#3	130.73(6)
O(10)#1-Eu(1)-O(14)	71.75(9)	O(1)-Eu(2)-O(12)#4	71.69(6)
O(2)-Eu(1)-Eu(2)	75.43(4)	O(1)-Eu(2)-O(5)	69.24(6)
O(2)-Eu(1)-O(1)	51.33(6)	O(1)-Eu(2)-O(11)#4	121.94(6)
O(2)-Eu(1)-O(5)	85.22(6)	O(4)#3-Eu(2)-Eu(1)	145.86(4)
O(2)-Eu(1)-O(6)	71.43(6)	O(12)#4-Eu(2)-Eu(1)	85.34(5)
O(2)-Eu(1)-N(3)#2	72.05(7)	O(12)#4-Eu(2)-O(4)#3	124.96(6)
O(6)-Eu(1)-Eu(2)	79.87(4)	O(12)#4-Eu(2)-O(5)	79.09(6)
O(6)-Eu(1)-O(1)	94.50(6)	O(5)-Eu(2)-Eu(1)	36.14(4)
O(6)-Eu(1)-N(3)#2	73.17(7)	O(5)-Eu(2)-O(4)#3	150.42(6)
O(13)-Eu(1)-Eu(2)	99.77(5)	O(3)#3-Eu(2)-Eu(1)	113.33(5)
O(13)-Eu(1)-O(1)	69.60(7)	O(3)#3-Eu(2)-O(1)	80.50(6)
O(13)-Eu(1)-O(5)	133.84(7)	O(3)#3-Eu(2)-O(4)#3	53.37(6)
O(13)-Eu(1)-O(2)	72.85(7)	O(3)#3-Eu(2)-O(12)#4	97.49(7)
O(13)-Eu(1)-O(6)	143.12(7)	O(3)#3-Eu(2)-O(5)	149.14(6)
O(13)-Eu(1)-N(3)#2	87.48(8)	O(3)#3-Eu(2)-O(11)#4	87.76(7)
N(3)#2-Eu(1)-Eu(2)	142.84(5)	O(11)#4-Eu(2)-Eu(1)	136.87(5)
N(3)#2-Eu(1)-O(1)	122.65(6)	O(11)#4-Eu(2)-O(4)#3	77.05(6)
O(14)-Eu(1)-Eu(2)	104.40(10)	O(11)#4-Eu(2)-O(12)#4	53.75(6)
O(14)-Eu(1)-O(1)	138.85(10)	O(11)#4-Eu(2)-O(5)	113.02(6)
O(14)-Eu(1)-O(5)	75.69(9)	Eu(2)-O(1)-Eu(1)	108.17(7)
O(14)-Eu(1)-O(2)	138.91(9)	Eu(2)-O(5)-Eu(1)	109.39(6)
O(14)-Eu(1)-O(6)	68.23(8)		

---

### 1-Tb

Tb(2)-O(6)	2.308(2)	Tb(1)-O(11)	2.280(2)
Tb(2)-O(10)#1	2.531(2)	Tb(1)-O(13)	2.406(2)
Tb(2)-O(9)	2.531(2)	Tb(1)-O(1)	2.496(2)
Tb(2)-O(3)	2.590(2)	Tb(1)-O(9)	2.412(2)
Tb(2)-O(12)	2.344(2)	Tb(1)-O(3)	2.402(2)
Tb(2)-O(4)	2.444(2)	Tb(1)-O(5)	2.288(2)
Tb(2)-O(7)	2.384(3)	Tb(1)-O(2)	2.360(2)
Tb(2)-O(8)	2.359(3)	Tb(1)-O(14)#1	2.409(2)
Tb(2)-N(3)#2	2.541(3)	O(6)-Tb(2)-O(10)#1	129.65(8)
O(6)-Tb(2)-O(9)	81.33(8)	O(8)-Tb(2)-O(10)#1	68.37(9)
O(6)-Tb(2)-O(3)	76.46(8)	O(8)-Tb(2)-O(9)	75.90(10)
O(6)-Tb(2)-O(12)	81.36(8)	O(8)-Tb(2)-O(3)	138.59(11)
O(6)-Tb(2)-O(4)	127.04(8)	O(8)-Tb(2)-O(4)	139.14(10)
O(6)-Tb(2)-O(7)	81.04(10)	O(8)-Tb(2)-O(7)	144.11(10)
O(6)-Tb(2)-O(8)	85.82(12)	O(8)-Tb(2)-N(3)#2	88.53(13)
O(6)-Tb(2)-N(3)#2	151.71(9)	N(3)#2-Tb(2)-O(3)	123.52(8)

O(6)-Tb(2)-C(23)#1	106.58(9)	O(11)-Tb(1)-O(13)	120.97(8)
O(6)-Tb(2)-C(5)#3	101.61(9)	O(11)-Tb(1)-O(1)	74.22(8)
O(10)#1-Tb(2)-O(3)	94.85(7)	O(11)-Tb(1)-O(9)	78.14(8)
O(10)#1-Tb(2)-N(3)#2	72.66(8)	O(11)-Tb(1)-O(3)	142.08(8)
O(10)#1-Tb(2)-C(23)#1	25.33(8)	O(11)-Tb(1)-O(5)	82.35(9)
O(10)#1-Tb(2)-C(5)#3	84.59(9)	O(11)-Tb(1)-O(2)	127.42(8)
O(9)-Tb(2)-O(10)#1	51.46(7)	O(11)-Tb(1)-O(14)#1	87.24(8)
O(9)-Tb(2)-O(3)	64.71(7)	O(13)-Tb(1)-O(1)	125.04(8)
O(9)-Tb(2)-N(3)#2	123.97(8)	O(13)-Tb(1)-O(9)	78.82(8)
O(12)-Tb(2)-O(10)#1	125.58(9)	O(13)-Tb(1)-O(14)#1	54.21(8)
O(12)-Tb(2)-O(9)	144.40(8)	O(9)-Tb(1)-O(1)	150.35(8)
O(12)-Tb(2)-O(3)	139.03(8)	O(3)-Tb(1)-O(13)	71.88(8)
O(12)-Tb(2)-O(4)	129.78(9)	O(3)-Tb(1)-O(1)	130.78(8)
O(12)-Tb(2)-O(7)	73.07(10)	O(3)-Tb(1)-O(9)	69.40(8)
O(12)-Tb(2)-O(8)	72.01(10)	O(3)-Tb(1)-O(14)#1	122.75(8)
O(12)-Tb(2)-N(3)#2	70.53(9)	O(5)-Tb(1)-O(13)	149.47(8)
O(4)-Tb(2)-O(10)#1	71.47(8)	O(5)-Tb(1)-O(1)	77.72(8)
O(4)-Tb(2)-O(9)	85.12(8)	O(5)-Tb(1)-O(9)	88.27(8)
O(4)-Tb(2)-O(3)	51.66(7)	O(5)-Tb(1)-O(3)	77.71(8)
O(4)-Tb(2)-N(3)#2	72.53(9)	O(5)-Tb(1)-O(2)	80.08(9)
O(7)-Tb(2)-O(10)#1	142.70(9)	O(5)-Tb(1)-O(14)#1	154.31(8)
O(7)-Tb(2)-O(9)	133.82(8)	O(2)-Tb(1)-O(13)	97.11(9)
O(7)-Tb(2)-O(3)	69.77(8)	O(2)-Tb(1)-O(1)	53.74(8)
O(7)-Tb(2)-O(4)	72.54(9)	O(2)-Tb(1)-O(9)	149.32(8)
O(7)-Tb(2)-N(3)#2	87.57(10)	O(2)-Tb(1)-O(3)	80.38(8)
O(14)#1-Tb(1)-O(1)	76.86(8)	O(2)-Tb(1)-O(14)#1	87.90(9)
O(14)#1-Tb(1)-O(9)	112.53(8)		

---

### 1-Gd

Gd(1)-Gd(2)	4.0680(5)	Gd(2)-O(12)#1	2.421(4)
Gd(1)-O(8)#1	2.545(4)	Gd(2)-O(2)	2.506(4)
Gd(1)-O(3)#2	2.612(4)	Gd(2)-O(1)	2.375(4)
Gd(1)-O(6)	2.314(4)	Gd(2)-O(11)#1	2.425(4)
Gd(1)-O(10)#3	2.372(4)	Gd(2)-O(5)	2.306(4)
Gd(1)-O(7)#1	2.574(4)	O(8)-Gd(1)#3	2.545(4)
Gd(1)-O(4)#2	2.472(4)	O(3)-Gd(1)#2	2.612(4)
Gd(1)-N(3)#4	2.556(5)	O(3)-Gd(2)#2	2.442(4)
Gd(1)-O(14)	2.378(5)	O(10)-Gd(1)#1	2.372(4)
Gd(1)-O(15)	2.412(5)	O(7)-Gd(1)#3	2.574(4)
Gd(2)-O(3)#2	2.442(4)	O(7)-Gd(2)#3	2.431(4)
Gd(2)-O(9)	2.296(4)	O(12)-Gd(2)#3	2.421(4)
Gd(2)-O(7)#1	2.431(4)	O(4)-Gd(1)#2	2.472(4)
O(8)#1-Gd(1)-Gd(2)	79.78(9)	O(11)-Gd(2)#3	2.425(4)
O(8)#1-Gd(1)-O(3)#2	94.63(13)	N(3)-Gd(1)#5	2.556(5)
O(8)#1-Gd(1)-O(7)#1	50.86(13)	O(15)-Gd(1)-O(4)#2	71.97(17)

O(8)#1-Gd(1)-N(3)#4	73.09(15)	O(15)-Gd(1)-N(3)#4	88.16(18)
O(3)#2-Gd(1)-Gd(2)	35.00(9)	O(3)#2-Gd(2)-Gd(1)	37.84(9)
O(6)-Gd(1)-Gd(2)	64.31(11)	O(3)#2-Gd(2)-O(2)	130.35(13)
O(6)-Gd(1)-O(8)#1	129.00(15)	O(9)-Gd(2)-Gd(1)	104.87(10)
O(6)-Gd(1)-O(3)#2	76.51(14)	O(9)-Gd(2)-O(3)#2	142.31(14)
O(6)-Gd(1)-O(10)#3	81.92(15)	O(9)-Gd(2)-O(7)#1	77.76(14)
O(6)-Gd(1)-O(7)#1	81.06(15)	O(9)-Gd(2)-O(12)#1	120.75(15)
O(6)-Gd(1)-O(4)#2	126.47(15)	O(9)-Gd(2)-O(2)	74.42(14)
O(6)-Gd(1)-N(3)#4	151.88(16)	O(9)-Gd(2)-O(1)	127.13(15)
O(6)-Gd(1)-O(14)	86.9(2)	O(9)-Gd(2)-O(11)#1	87.04(15)
O(6)-Gd(1)-O(15)	81.00(19)	O(9)-Gd(2)-O(5)	82.54(15)
O(10)#3-Gd(1)-Gd(2)	146.23(10)	O(7)#1-Gd(2)-Gd(1)	36.83(9)
O(10)#3-Gd(1)-O(8)#1	126.06(15)	O(7)#1-Gd(2)-O(3)#2	70.23(13)
O(10)#3-Gd(1)-O(3)#2	138.65(15)	O(7)#1-Gd(2)-O(2)	150.38(14)
O(10)#3-Gd(1)-O(7)#1	144.57(15)	O(12)#1-Gd(2)-Gd(1)	85.66(10)
O(10)#3-Gd(1)-O(4)#2	129.33(15)	O(12)#1-Gd(2)-O(3)#2	72.17(14)
O(10)#3-Gd(1)-N(3)#4	70.09(15)	O(12)#1-Gd(2)-O(7)#1	78.63(15)
O(10)#3-Gd(1)-O(14)	71.60(18)	O(12)#1-Gd(2)-O(2)	124.84(15)
O(10)#3-Gd(1)-O(15)	73.22(17)	O(12)#1-Gd(2)-O(11)#1	53.20(14)
O(7)#1-Gd(1)-Gd(2)	34.47(9)	O(2)-Gd(2)-Gd(1)	145.83(10)
O(7)#1-Gd(1)-O(3)#2	65.42(12)	O(1)-Gd(2)-Gd(1)	113.41(10)
O(4)#2-Gd(1)-Gd(2)	75.63(10)	O(1)-Gd(2)-O(3)#2	80.09(14)
O(4)#2-Gd(1)-O(8)#1	71.84(15)	O(1)-Gd(2)-O(7)#1	149.82(14)
O(4)#2-Gd(1)-O(3)#2	50.98(13)	O(1)-Gd(2)-O(12)#1	97.78(16)
O(4)#2-Gd(1)-O(7)#1	85.41(14)	O(1)-Gd(2)-O(2)	53.36(14)
O(4)#2-Gd(1)-N(3)#4	73.13(15)	O(1)-Gd(2)-O(11)#1	89.54(16)
N(3)#4-Gd(1)-Gd(2)	143.57(11)	O(11)#1-Gd(2)-Gd(1)	136.04(10)
N(3)#4-Gd(1)-O(3)#2	123.44(15)	O(11)#1-Gd(2)-O(3)#2	122.34(14)
N(3)#4-Gd(1)-O(7)#1	123.85(14)	O(11)#1-Gd(2)-O(7)#1	110.67(14)
O(14)-Gd(1)-Gd(2)	105.35(17)	O(11)#1-Gd(2)-O(2)	78.02(14)
O(14)-Gd(1)-O(8)#1	68.36(16)	O(5)-Gd(2)-Gd(1)	67.94(11)
O(14)-Gd(1)-O(3)#2	140.31(19)	O(5)-Gd(2)-O(3)#2	77.26(14)
O(14)-Gd(1)-O(7)#1	76.64(18)	O(5)-Gd(2)-O(7)#1	88.33(15)
O(14)-Gd(1)-O(4)#2	139.18(17)	O(5)-Gd(2)-O(12)#1	149.27(15)
O(14)-Gd(1)-N(3)#4	86.9(2)	O(5)-Gd(2)-O(2)	78.24(15)
O(14)-Gd(1)-O(15)	144.02(18)	O(5)-Gd(2)-O(1)	79.71(16)
O(15)-Gd(1)-Gd(2)	99.60(13)	O(5)-Gd(2)-O(11)#1	155.88(15)
O(15)-Gd(1)-O(8)#1	142.72(17)	Gd(2)#2-O(3)-Gd(1)#2	107.16(14)
O(15)-Gd(1)-O(3)#2	68.89(15)	Gd(2)#3-O(7)-Gd(1)#3	108.71(15)
O(15)-Gd(1)-O(7)#1	133.59(16)		

---

**1-Eu:** #1 -x+1/2,y-1/2,-z+1/2; #2 -x+1,-y+1,-z+1; #3 -x+1,y,-z+1/2; #4 -x+1/2,y+1/2,-z+1/2; **1-Tb:** #1 -x+3/2,y-1/2,-z+1/2; #2 x,-y+1,z-1/2; #3 -x+1,y,-z+1/2; #4 -x+3/2,y+1/2,-z+1/2; #5 x,-y+1,z+1/2; **1-Gd:** #1 -x+1/2,y+1/2,-z+3/2; #2 -x+1,y,-z+3/2; #3 -x+1/2,y-1/2,-z+3/2; #4 x,-y+1,z+1/2; #5 x,-y+1,z-1/2;

**Table S2.** Summary of the quantum yields of the reported white-light-emission doped MOFs.

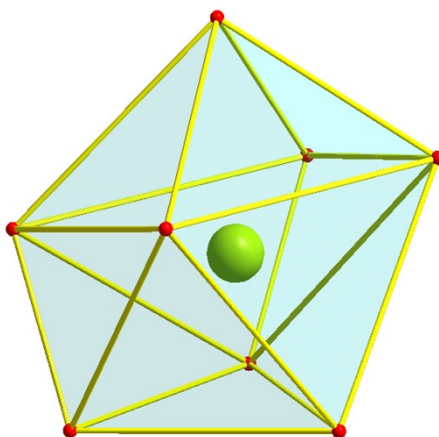
Complex	Quantum yield	Ref.
La <sub>0.6</sub> Eu <sub>0.1</sub> Tb <sub>0.3</sub> -BTPCA	47.33 %	1
Eu <sub>0.005</sub> Tb <sub>0.995</sub> -BTPCA	46.15 %	
Eu <sub>0.01</sub> Gd <sub>0.6015</sub> Tb <sub>0.3885</sub>	36.49 %	<b>This work</b>
Eu <sub>0.0855</sub> Gd <sub>0.6285</sub> Tb <sub>0.2860</sub>	22.4 %	2
HMA-Tb <sub>10</sub> Eu <sub>1</sub>	11.41 %	3
0.5% Eu <sup>3+</sup> -doped 2-Tb	11.4 %	4

**Table S3.** The quenching constants of **1-Eu** and reported MOFs for NB.

Complex	Quenching Constants (K <sub>SV</sub> /M <sup>-1</sup> )	Ref.
[Cd(TPA)(DIB)](n)	1.7 × 10 <sup>4</sup>	5
[Zn <sub>2</sub> (4,4'-nba) <sub>2</sub> (1,4-bib) <sub>2</sub> ] <sub>n</sub>	1.59 × 10 <sup>4</sup>	6
{[Eu <sub>2</sub> (L) <sub>3</sub> ·DMF·H <sub>2</sub> O]·DMF·H <sub>2</sub> O} <sub>n</sub>	1.5143 × 10 <sup>4</sup>	<b>This work</b>
{MgL(H <sub>2</sub> O) <sub>2</sub> } <sub>n</sub>	1.07 × 10 <sup>4</sup>	7
Ln <sub>2</sub> (NSBPDC) <sub>3</sub> (H <sub>2</sub> O) <sub>4</sub> ·x(H <sub>2</sub> O)	6.5512 × 10 <sup>3</sup>	8
Zn <sub>3</sub> (BTC) <sub>2</sub> : Eu(III)	3.957 × 10 <sup>3</sup>	9
[Zn(H <sub>2</sub> L <sup>2-</sup> )(H <sub>2</sub> O)] <sub>n</sub>	3.26 × 10 <sup>3</sup>	10
{[Zn(L)](DMF) <sub>3</sub> } <sub>n</sub>	2.875 × 10 <sup>3</sup>	11

**Table S4.** Results of ICP Analyses of Eu<sup>3+</sup>.

Samples	Concentration of Eu <sup>3+</sup> (ppb)
NB@CH <sub>3</sub> OH	6.375
Filter liquor of recycle <b>1-Eu</b>	6.813

**Figure S1. (a)** A distorted trigondodecahedron geometry.

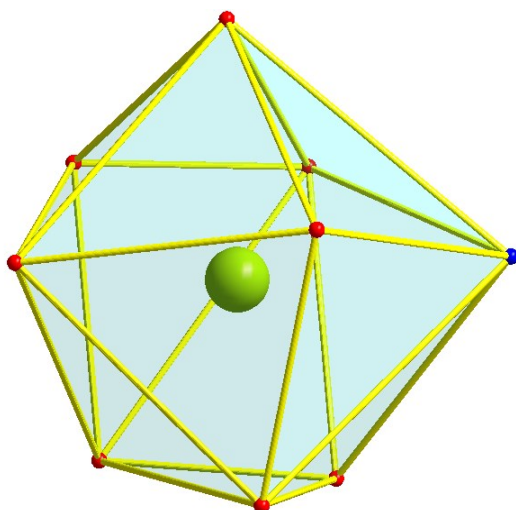


**Figure S1. (b)** A distorted tetrakaidecahedron geometry.

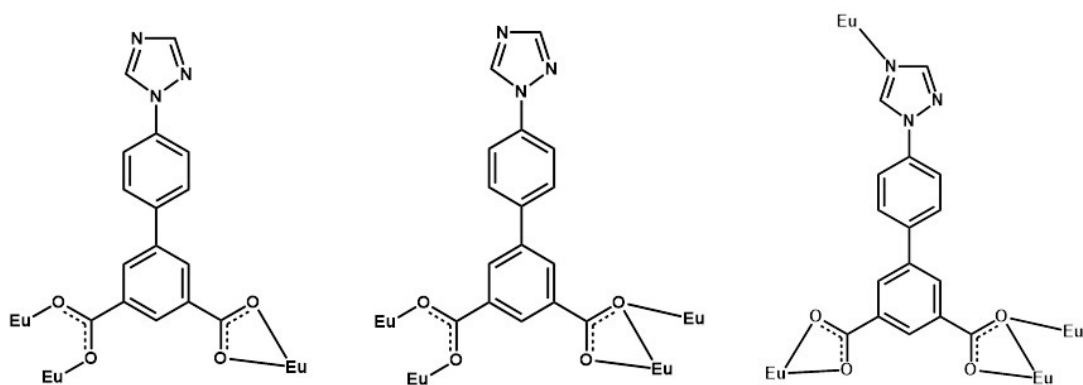


**Figure S2.** Three coordination modes of  $L^{2-}$  in **1-Eu**, ( $\eta^2\mu_2\chi^2$ ,  $\eta^2\mu_1\chi^2$  and  $\eta^2\mu_2\chi^3$ ).

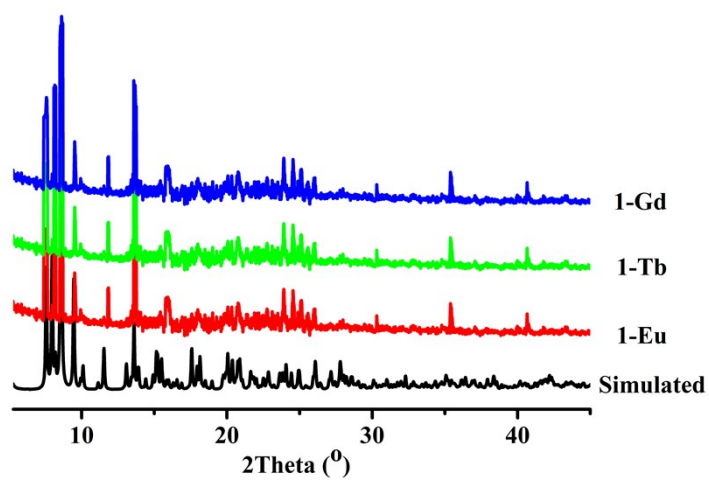


**Figure S3.** PXRD patterns of **1-Eu** simulated from the X-ray single-crystal structure and as-synthesized samples of **1-Eu**, **1-Tb** and **1-Gd**.



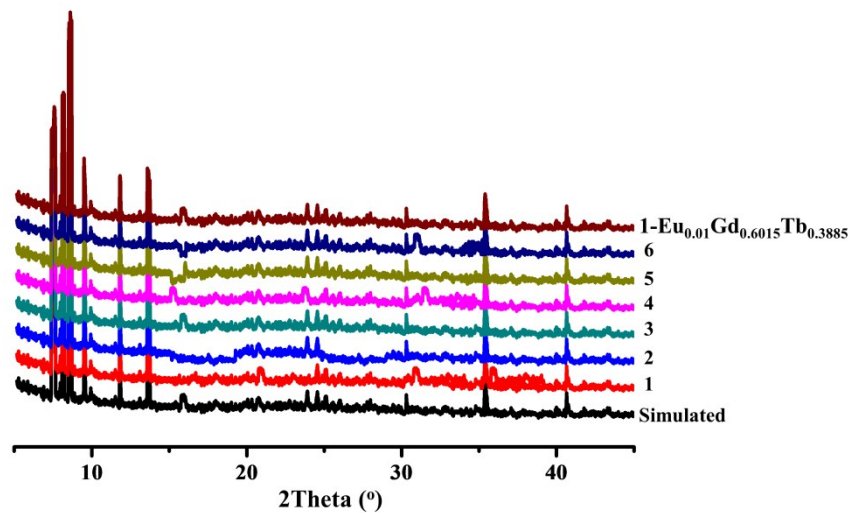


Figure S4. PXRD patterns of doped samples.

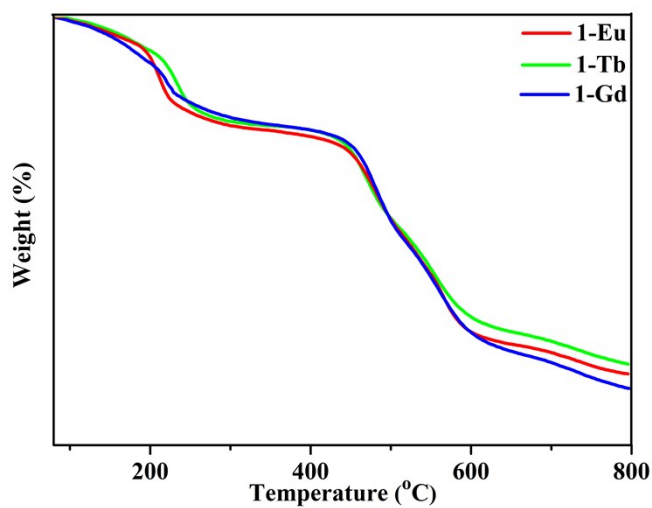


Figure S5. The TGA plots of 1-Eu, 1-Tb and 1-Gd under N<sub>2</sub> environment.

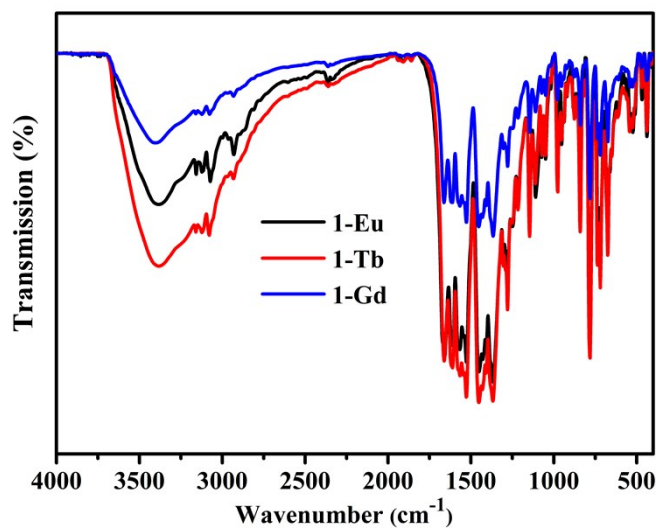
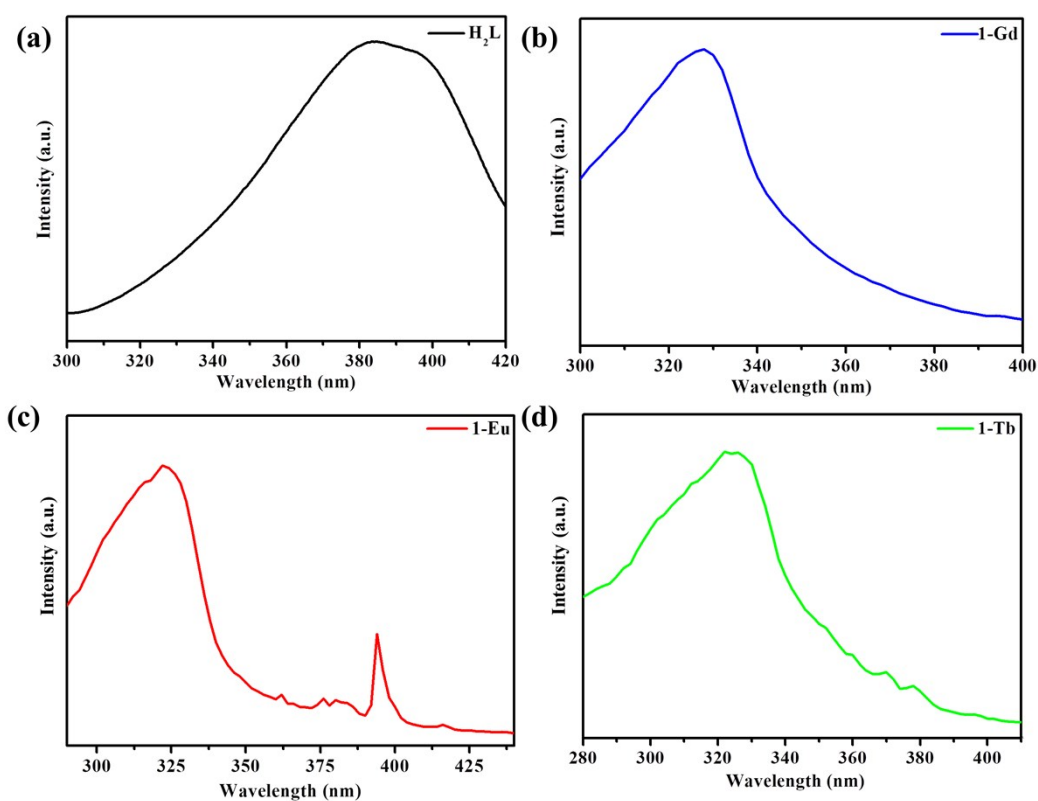
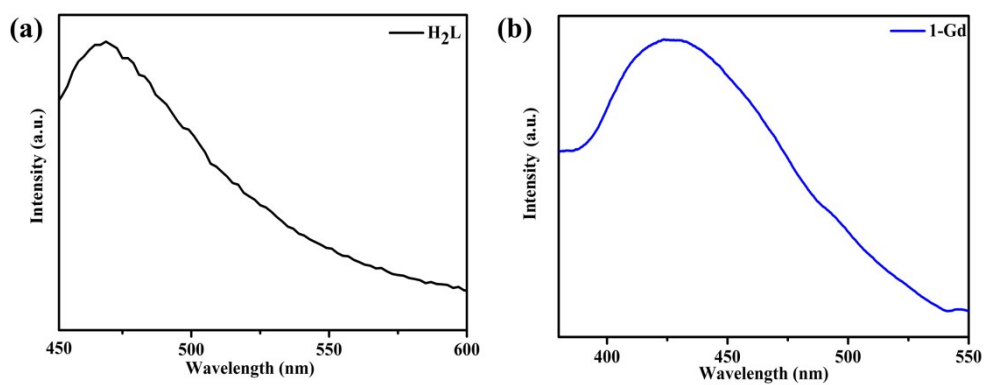


Figure S6. The FT-IR spectrometer of 1-Eu, 1-Tb and 1-Gd.



**Figure S7.** Solid state excitation spectra of  $H_2L$  (a),  $1-Gd$ (b),  $1-Eu$ (c) and  $1-Tb$ (d).



**Figure S8.** Solid-state emission spectra of  $H_2L$ (a),  $1-Gd$  (b).

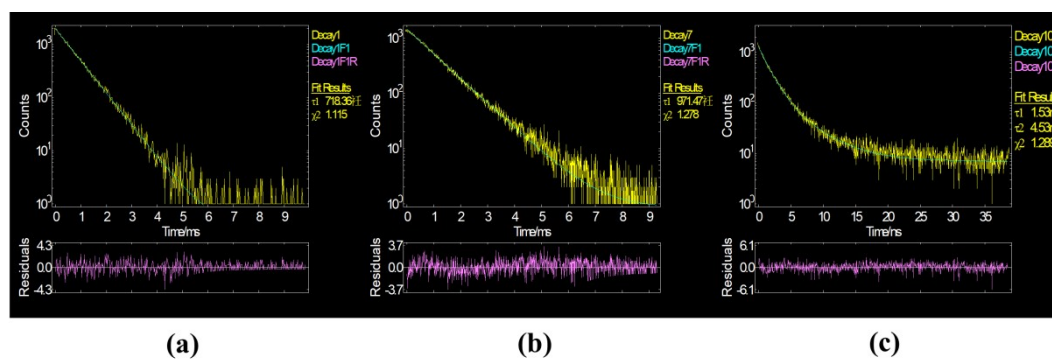


**Figure S9.** Luminescence decay lifetimes of  $1-Eu$  (a),  $1-Tb$  (b) and  $1-Gd$  (c) measured at the excitation.

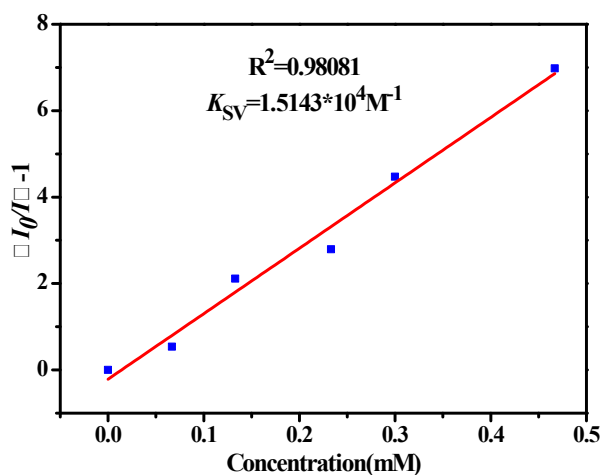


**Figure S10.** Linear correlation for the plot of  $(I_0/I)-1$  vs concentration of nitrobenzene in low concentration range.

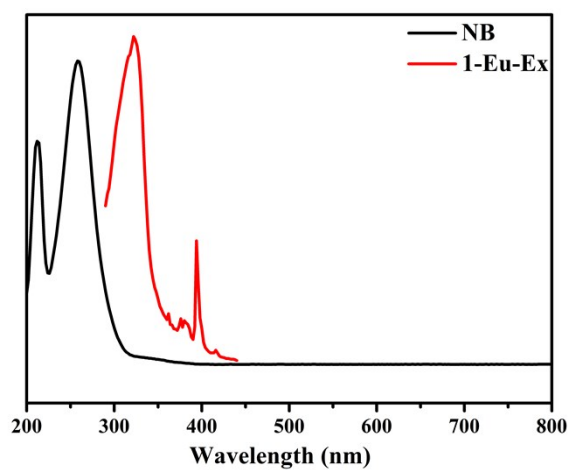


**Figure S11.** UV-Vis adsorption spectra of nitrobenzene in  $\text{CH}_3\text{OH}$  solution and excitation spectrum of **1-Eu** in  $\text{CH}_3\text{OH}$  solution.

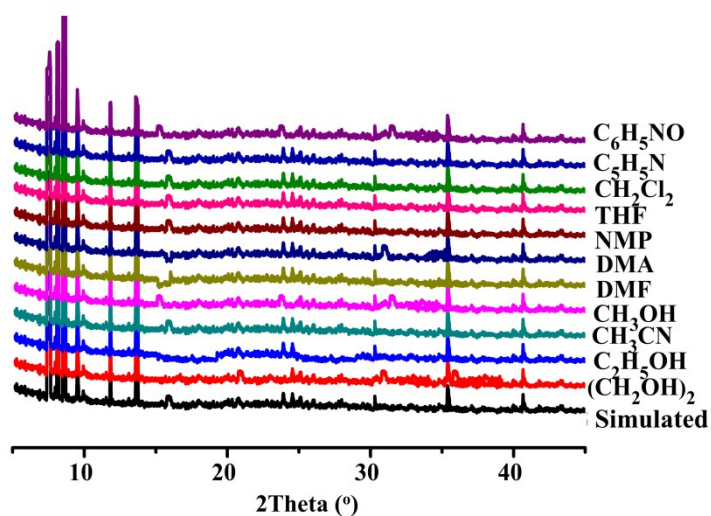


**Figure S12.** The PXRD patterns of **1-Eu** treated by small organic molecules solutions.

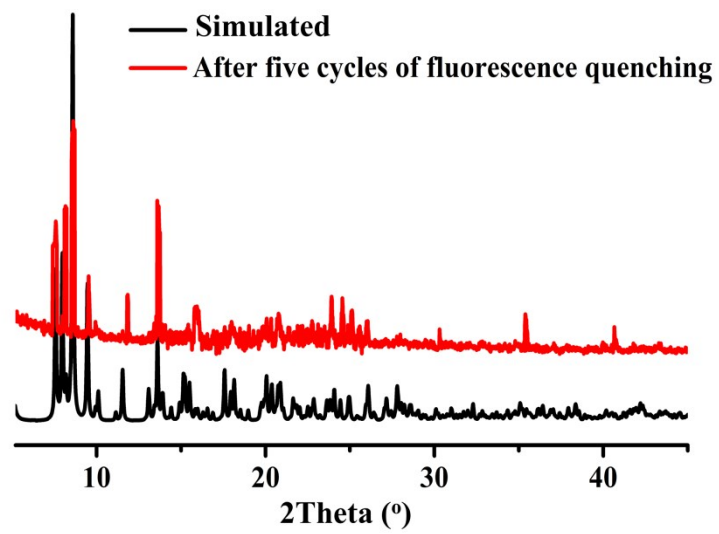


**Figure S13.** The PXRD patterns of 1-Eu treated by multi-cycle fluorescence quenching.

## References:

1. Q. Tang, S. Liu, Y. Liu, D. He, J. Miao, X. Wang, Y. Ji and Z. Zheng, Color tuning and white light emission via in situ doping of luminescent lanthanide metal-organic frameworks, *Inorg. Chem.*, 2014, **53**, 289-293.
2. X.-Y. Li, W.-J. Shi, X.-Q. Wang, L.-N. Ma, L. Hou and Y.-Y. Wang, Luminescence Modulation, White Light Emission, and Energy Transfer in a Family of Lanthanide Metal-Organic Frameworks Based on a Planar  $\pi$ -Conjugated Ligand, *Cryst. Growth Des.*, 2017, **17**, 4217-4224.
3. H. Liu, T. Chu, Z. Rao, S. Wang, Y. Yang and W.-T. Wong, The Tunable White-Light and Multicolor Emission in An Electrodeposited Thin Film of Mixed Lanthanide Coordination Polymers, *Adv. Opt. Mater.*, 2015, **3**, 1545-1550.
4. Z.-F. Liu, M.-F. Wu, S.-H. Wang, F.-K. Zheng, G.-E. Wang, J. Chen, Y. Xiao, A. Q. Wu, G.-C. Guo and J.-S. Huang, Eu<sup>3+</sup>-doped Tb<sup>3+</sup> metal-organic frameworks emitting tunable three primary colors towards white light, *J. Mater. Chem. C*, 2013, **1**, 4634-4639.
5. X. Wang, Y. Han, X. X. Han, X. Hou, J.-J. Wang and F. Fu, Highly selective and sensitive detection of Hg<sup>2+</sup>, Cr<sub>2</sub>O<sub>7</sub><sup>2-</sup>, and nitrobenzene/2,4-dinitrophenol in water via two fluorescent Cd-CPs, *New J. Chem.*, 2018, **42**, 19844-19852.
6. T.-Y. Xu, J.-M. Li, Y.-H. Han, A.-R. Wang, K.-H. He and Z.-F. Shi, A new 3D four-fold interpenetrated dia-like luminescent Zn(II)-based metal-organic framework: the sensitive detection of Fe<sup>3+</sup>, Cr<sub>2</sub>O<sub>7</sub><sup>2-</sup>, and CrO<sub>4</sub><sup>2-</sup> in water, and nitrobenzene in ethanol, *New J. Chem.*, 2020, **44**, 4011-4022.
7. Y. S. Xue, W. Cheng, J. P. Cao and Y. Xu, 3D Enantiomorphic Mg-Based Metal-Organic Frameworks as Chemical Sensor of Nitrobenzene and Efficient Catalyst for CO<sub>2</sub> Cycloaddition, *Chem-Asian J.*, 2019, **14**, 1949-1957.
8. L.-L. Ren, Y.-Y. Cui, A.-L. Cheng and E.-Q. Gao, Water-stable lanthanide-based metal-organic frameworks for rapid and sensitive detection of nitrobenzene derivatives, *J. Solid State Chem.*, 2019, **270**, 463-469.
9. S. Xian, H.-L. Chen, W.-L. Feng, X.-Z. Yang, Y.-Q. Wang and B.-X. Li, Eu(III) doped zinc metal organic framework material and its sensing detection for nitrobenzene, *J. Solid State Chem.*, 2019, **280**, 120984.
10. Q. Zhao and C.-D. Si, A Novel Zinc Luminescent Coordination Polymer Based on a Tetracarboxylate Acid Ligand for the Detection of Nitrobenzene, *Cryst. Res. Technol.*, 2019, **54**, 1800155.
11. L. Wei, J. Lou, L. Liu, X.-Z. Ma, J. Li, R. Pan and Y.-X. Zhang, Zn(II)-Containing Metal-Organic Framework for Fluorescence Detection of Nitrobenzene and Prevention Effect on Hypertension via Down-Regulating the Expression of Vitamin D Receptor, *J. Clust. Sci.*, 2019, **31**, 479-486.